Available online at www.sciencedirect.com
SCIENCE DIRECT
Polymer 47 (2006) 2555–2563
polymer
www.elsevier.com/locate/polymer

Modelling cantilever-based force spectroscopy with polymers

Ferdinand Kühner *, Hermann E. Gaub

Lehrstuhl fur Angewandte Physik and Center for NanoScience, Ludwig-Maximilians-Universitat, Amalienstrabetae 54, Munchen 80799, Germany

Received 29 November 2005; received in revised form 6 December 2005; accepted 8 December 2005
Available online 8 February 2006

Abstract

Polymers play a central role in cantilever-based single molecule force spectroscopy, either as sample or as anchor of the molecular complexes under investigation. Here we investigated the role of the polymer for the coupling of thermal and mechanical fluctuations of the cantilever into the molecular complex under investigation. We first analyzed the low pass characteristics of the polymeric anchor as a function of its length and identified the optimum filter characteristics for its applications in bond rupture investigations. We then studied the propagation of mechanical fluctuations of either cantilever or anchor point via the polymer into the molecular complex under investigation. With model calculation based on measured polymer extensibilities we were able to identify the optimum combination of cantilever stiffness and anchor length for a given bond strength of the molecular complex to be investigated and to estimate the resulting resolution limit of the different combinations.

Keywords: Cantilever; Optimum bandwidth filter; Resolution limit of dynamic force

1. Introduction

Highly dynamic processes between individual molecules or molecular complexes characterize biological systems. Where in the past such processes were investigated in the ensemble, either kinetically or in thermodynamic equilibrium, single molecule techniques nowadays provide access to the response of the individual constituents. Conformational changes as a result of external forces, which are applied to the molecular entities under investigation, are probes with unparalleled resolution and sensitivity. Parameters such as the potential width, the length of the interaction, the kinetic rates or the elastic properties (conformational changes) of the molecular system are derived in such experiments [1,2].

Up to date, a broad variety of systems was successfully investigated with these techniques: the unfolding and refolding pattern of cytosolic proteins like titin [3,4] or as well as membrane bound proteins like bacteriorhodopsin was measured [5–7], several ligand–receptor complexes were studied [8–12] and the mechanics of the supramolecular arrangements of DNA were clarified [13,14].

In all these examples, polymers played a crucial role either as subject of the investigation or as essential requisite, e.g. as elastic coupler to either the sample surface or the cantilever [9]. Their mechanical properties have, therefore, been in the focus of many studies and a great deal [15] of new information was obtained by both single molecules force spectroscopy [16] and also by modelling [17].

2. Results and discussion

Cantilever and polymer act as a nano-mechanical unit in a temperature bath and so thermal fluctuations are the result. Under optimum conditions state of the art instruments are limited in their resolutions by these thermal fluctuations. However, also mechanical fluctuations may couple into the instrument and propagate through the polymeric anchors into the molecular complex under investigation. These fluctuations will modulate the unbinding process and thus alter the measured unbinding forces. Since many biologically relevant processes occur close to the resolution limit, a thorough analysis of the detection limit was carried out with the scope to develop adequate strategies for a further improvement of this technique.

Cantilevers of different geometry and stiffness show different thermal excitation spectra despite the fact that in each case they are driven by k_BT. Different cantilevers may, therefore, be chosen for different applications accordingly. Time resolved measurements, e.g. stretching of a polymeric anchor followed by the rupture of a molecular complex, require

* Corresponding author. Tel.: +49 89 2180 2005; fax: +49 89 2180 2050.
E-mail address: ferdinand.Keuhner@physik.uni-Muenchen.de (F. Kühner).

0032-3861/$ - see front matter © 2006 Elsevier Ltd. All rights reserved.
doi:10.1016/j.polymer.2005.12.090

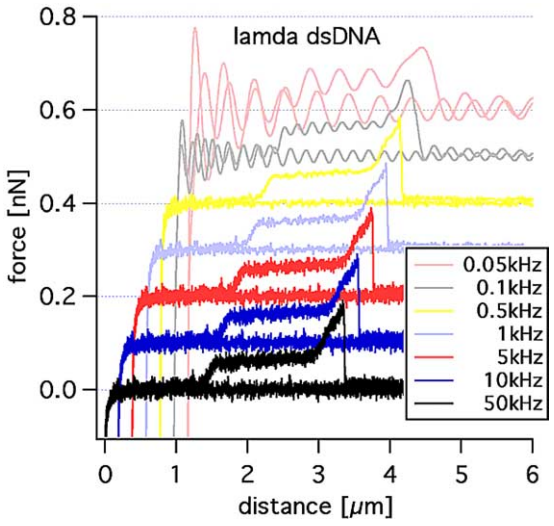

Fig. 1. Force extension traces of lambda DNA. Applying different low-pass filters on the data leads to a reduction of noise in the measured force curves. In the diagram low-pass filters with different corner frequencies—ranging from 10 to 0.05 kHz—were applied. The noise in the force curves is reduced drastically when the corner frequency of the filter approaches the resonance frequency of the cantilever. If the corner frequency is chosen too low, (e.g. grey curve, 0.1 kHz filter) relevant information, particularly on the rupture event is lost.

a suitable reduction of the bandwidth in order to extract the relevant information from the measured signal.

In the following the typical intrinsic noise values for different cantilevers were evaluated and the limits of their detection possibilities in certain bandwidths are calculated and compared with the experiments. Additionally, the bandwidth of a rupture event was calculated and based on the bandwidth distribution, the optimum filter frequencies were determined.

A typical example of such a single molecule force spectroscopy experiment is given in Fig. 1. Here a dsDNA strand [13] on the surface was picked up by the cantilever tip and extended. The graph shows the force response of a double stranded DNA upon stretching. When the DNA is relaxed, only thermal fluctuations cause an increase in the end-to-end distance, the resulting cantilever deflections do not exceed the noise floor. However, when the end-to-end distance of the polymer approaches the contour length, which in this example occurs at roughly 1.5 μm, the counteracting forces become significant. At a force of approximately 65 pN the double stranded DNA undergoes a phase transition resulting in an extended plateau of the force. At the end of this transition, the backbone of the DNA is stretched resulting in a steep increase in the force upon further extension. At a force of roughly 200 pN the DNA detaches from the tip, which results in a sharp drop of the force. In this experiment shown here, the cantilever was retracted with a speed of 16 μm per second and the deflection signal was sampled with 50 kHz. The cantilever itself had a resonant frequency of 2.5 kHz and a spring constant of 20 pN/nm.

This curve makes evident that a suitable filter is needed to improve the signal to noise ratio in the plateau region without camouflaging the rupture event with its sharp edge. The reduction in the signal bandwidth has to be in a delicate balance.

The colored traces in Fig. 1 show the same data, but filtered in the frequency domain with different bandwidths. The reduction of the corner frequency of the low-pass filter below 5 kHz results first in a significant smoothing and at a reduction below 500 Hz marked distortions of the signal and also to a non-tolerable information loss, particularly in the range of the bond rupture. Obviously the system itself acts as a low-pass filter. As we will learn later, it is the corner frequency of the viscous damped cantilever, which limits the bandwidth of the signal in the first place.

3. Thermal noise spectrum of a cantilever in solution

In Fig. 2(a) a typical power density spectrum (PSD) of the thermally excited cantilever deflection is given. The most remarkable feature of this spectrum is that it is not dominated by $1/f$ decay, rather by over damped resonances of the cantilever. This confirms our previous statement that with state of the art instrumentation the resolution limit of cantilever-based force spectroscopy is not determined by electronic noise (Johnson noise), but by thermal noise of the cantilever [18].

In the following we use the expression thermal noise for that part of the measured signal, which was caused by thermal fluctuations. Later on we will use the term mechanical noise and refer with this expression to that part in the signal, which is caused by mechanically induced fluctuations (e.g. by sound).

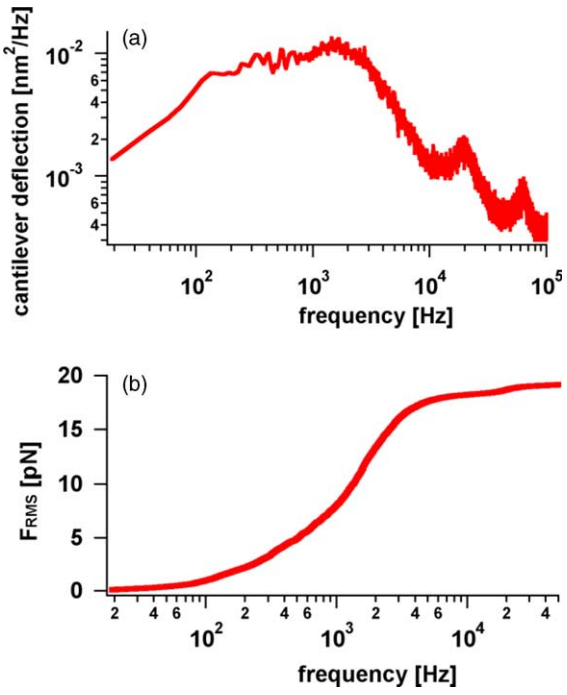

Fig. 2. (a) Power density spectrum (PSD) of the thermal fluctuation of the cantilever deflection. The spectrum is dominated by the mechanical resonances (fundamental at 2.5 kHz) rather than by $1/f$ noise. (b) Integrated thermal cantilever noise as a function of the bandwidth (Eq. (1)). The rote means square of the noise increases mainly at the resonant frequencies of the cantilever.

The spectrum in Fig. 2(a) was integrated to derive the root mean square of the force fluctuations:

$$F_{\mathrm{RMS}} = \sqrt{\int_{f_1}^{f_2} F(f)^2 \mathrm{d}f} \tag{1}$$

The square root of the integrated power spectrum of the cantilever equals the frequency dependent noise average [19]. The frequency range between f_2 and f_1 is referred to as the 'measurement bandwidth'. The result is shown in Fig. 2(b). At the resonant frequency of the cantilever (here at 2.5 kHz) the noise increases most dramatically. It also shows that the thermal energy is predominantly dissipated at the resonant frequencies of the cantilever.

Cantilevers relevant for biological force measurements have resonant frequencies from 0.3 to 10 kHz in water. The high damping by the water results in a low Q (quality factor) of the resonances. By using smaller cantilevers this damping can be minimized and the resonance frequencies can be shifted to higher values. In the measurement bandwidth, therefore, the signal to noise ratio (SNR) can be optimized by separating the high-frequency noise from the lower frequency components, which compose the force ramp in an unbinding experiment.

An oscillating force $F(\nu)$ to be measured (e.g. Fourier component of a certain time-dependent force) will be camouflaged by the thermal fluctuations of the cantilever [18]. The resulting signal to noise ratio is given by

$$\mathrm{SNR} = \frac{\frac{F(\nu)}{k} G(\nu)}{\sqrt{\frac{4k_{\mathrm{B}}TRB}{k^2} G^2(\nu) + (\text{instrument noise})^2}} \tag{2}$$

where k_{B} is the Boltzmann's constant, T the temperature, k the cantilever spring constant[1] and $G(\nu)$ the frequency dependent response function. The first term in the denominator is thermal noise as described by the fluctuation–dissipation theorem, which requires any system that has energy dissipation R, to also experience fluctuations. Assuming negligible instrumental noise, this expression can be further simplified and yields to the minimum detectable force, at a SNR of 1:

$$F_{\mathrm{min}} = \sqrt{4k_{\mathrm{B}}TRB} \tag{3}$$

As can be seen from Eq. (3), the minimum detectable force at a fixed bandwidth B can either be lowered by minimizing viscous damping R, or by lowering the temperature of the experiment.

Since both parameters may not be altered in biologically relevant ambient conditions, the only method to increase the resolution limit is to use smaller cantilevers. Unfortunately, the cantilever size is limited by the optical detection and, therefore, by optical diffraction. However, the theoretical limit of detecting the displacement of the cantilever is given by [20]

$$\mathrm{SNR} = \sqrt{\frac{\lambda\eta P_{\mathrm{tot}}}{2hcB}} g_1 g_2 \frac{\pi}{2} \frac{w_0}{l} \frac{\Delta z}{\lambda} \tag{4}$$

where P_{tot} is the total optical power incident on the photo detector, η the quantum efficiency of the detector, h Plancks constant, c speed of light in air, B the bandwidth of the detection system, w_0 the spot diameter on the cantilever, Δz the displacement of the cantilever, l the length of cantilever and g_1, g_2 the quality factor of the Gaussian shape of the beam.

For typical values and a SNR of 1 the equation results in

$$\Delta z \approx 10^{-14} \frac{l}{w_0} [m] \tag{5}$$

As can be seen from these considerations, shorter cantilevers result in a better deflection resolution, however, the need to focusing the laser beam counteracts.

4. Bandwidth limit for polymer extension

The time course of the experiment and so the frequencies to be recovered from the measured signal dictate the choice of the measurement bandwidth. Commercial instruments typically use a 1 kHz filter or alternatively a smoothing factor [21], which also results in a low-pass filter. However, in certain cases this measurement bandwidth is too narrow and cuts off relevant information of the signal or to broad and results in an unpleasant SNR.

Typical speeds for the cantilever range between 10 nm/s and up to 20 μm/s. The lower value is limited by drift, the upper by hydrodynamic drag. Most experiments employ a polymer spacer at the cantilever to avoid the direct coupling of fluctuations of the cantilever into the examined sample. Additionally, with the use of spacers the unbinding event does not occur directly at the surface, reducing the influence of force fields from cantilever and substrate. Furthermore, the known spacer length allows the discrimination between unspecific surface interaction and receptor–ligand interaction, by characterising the elastic response of the polymer spacer in a well-defined distance window. An attachment not to the point rather to apex of the cantilever tip will result in a shift of the force curve towards shorter lengths. In cases the polymer length is known this can be corrected. Last but not least: by analysing the elasticity of the polymer spacer it is possible to differentiate single molecule unbinding events from multiple interactions.

The extension of such a polymer spacer can be simulated with a WLC-model, which is truncated at higher extensions to account for the rupture event (Fig. 3(a)). The bond rupture and the following relaxation of the cantilever, which is dampened by hydrodynamic friction, is modelled by a exponential decay with a relaxation time between 200 and 800 μs, adjusted for the specific cantilever. No explicit thermal fluctuations were taken into account so far.

Fig. 3(b) shows the power density spectrum (PSD) of the trace in Fig. 3(a). As can be seen from this graph, a 50 nm long

[1] Spring constant $k = (1/4)Eb(d^3/l^3)$, E, Young's modulus; b, width; d, thick; l, length.

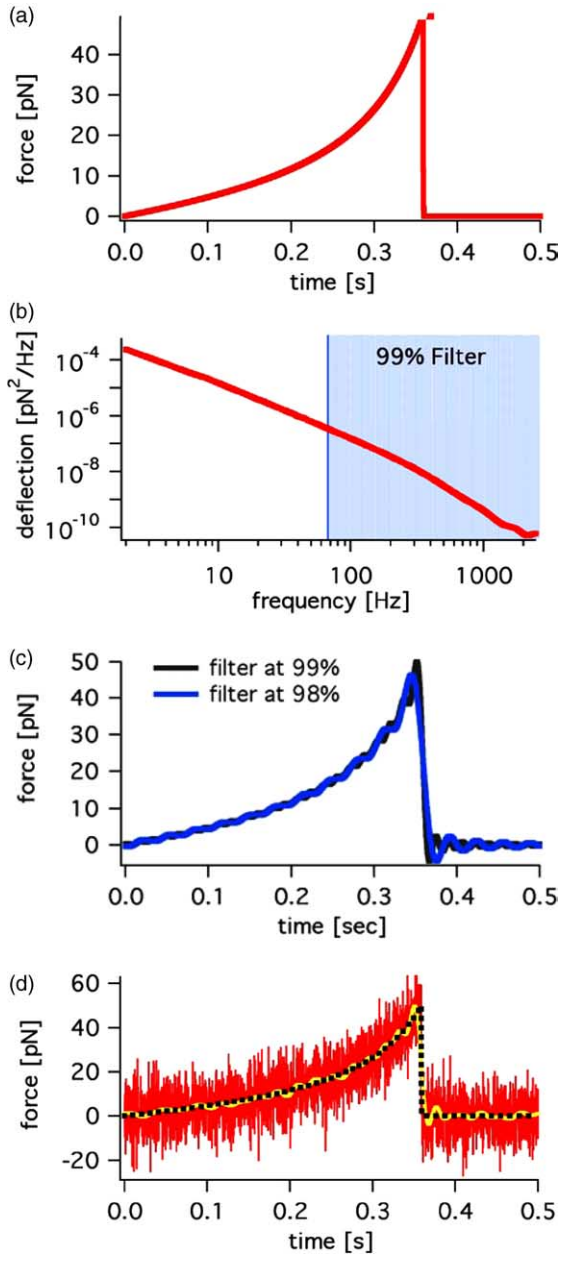

Fig. 3. (a) Computer-generated force curve of a 50 nm long polymer with a persistence length of 3 Å based on the WLC function with a retrace speed of 100 nm/s. The rupture event is simulated at 50 pN by an exponential decay, which models the damping of the cantilever by hydrodynamic friction. (b) PSD of the computer-generated force curve in (a). The force curve can be fully described in the bandwidth window of 0–1 kHz. (c) Force curves filtered such that 98 or 99% of the signal in the frequency domain remains. The force peak is reduced by 10 and 2%, respectively. (d) Model curves extended by thermal noise. Applying the 99% filter of (b) results in the yellow curve, which recovers the original noise free black trace in an optimum manner.

polymer spacer, with a persistence length of 3 Å, pulled at a speed of 0.1 μm/s can be fully described in the bandwidth window of 0–1 kHz. Faster speeds or shorter polymers shift the spectrum towards higher frequencies and as a result a higher bandwidth will be required. The shaded cut off line is drawn such that 99% of the PSD signal (note the logarithmical scale) is retained, if the upper limit of the bandwidth were reduced.

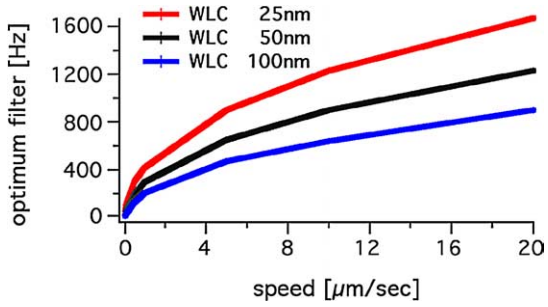

Fig. 4. Optimum bandwidth filter for different speeds and different polymer lengths. The SNR is greatly improved by using a monodisperse polymeric spacer.

The resulting distortions of the signal in the time domain is demonstrated for either a reduction to 99 or 98% in Fig. 3(c). Since the rupture force in the case of the 99% reduction is modified only by less than 2%, whereas a reduction to 98% already results in a 10% error, a bandwidth reduction to a value of 99% seems to be a desirable compromise.

In Fig. 3(d) this model was expanded by adding thermal noise. Applying the bandwidth cut-off corresponding to the 99% criteria results in the yellow curve, which recovers the original noise free black trace in an optimum manner.

Since pulling speed and polymer length have a reverse effect on the optimum bandwidth, we analyzed this relation and plotted it in Fig. 4. The upper cut-off frequency of the filter is plotted here as a function of the pulling speed for different polymer lengths. As can be seen, the use of monodisperse polymeric anchors may greatly improve the signal to noise ratio of the measurement, since the filters may be adjusted precisely.

5. Force resolution limits of different cantilevers

With this framework set out the resolution limits for detecting rupture events via polymer spacers were determined for different cantilevers. For this purpose an artificial data set of force curves with rupture events via polymer spacers were generated in the computer (Fig. 5). The added noise was specifically attenuated to the characteristic values of the different cantilevers.

This artificial data set was analysed and compared with the initial input values, which where used to create the data. This modelling procedure allows to optimize the analysis method and also the resolution limit. In the simulation, the rupture events were modelled by a WLC-function, analog Fig. 3(a). Typical noise values were generated on the basis of the power spectrum of a cantilever in liquid. These noise values were added to the force curves with the rupture events. The resulting traces were filtered as described above, by applying a certain frequency cut-off.

These artificial data sets were analyzed in an automated routine, which searches the minima of the differentiated force curve to evaluate the location of the rupture event. The maximum force value (signal) at this location plus the history before the maximum are compared with the noise. This defines the SNR ratio with which this event is detected. This SNR is

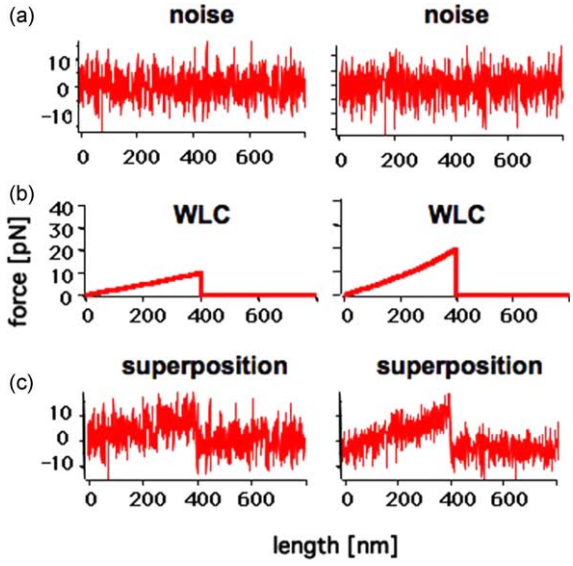

Fig. 5. Simulation steps for artificial data set of force curves with different interactions. (a) A typical PSD of a cantilever is translated into a noise time scale. (b) Secondly, an interaction is simulated by a WLC function. (c) The superposition of both curves results in an artificial force curve.

used as criteria for the discrimination of 'true positive' events from noise. An operational threshold value is adjusted by gradually rising the threshold until 0.1% of rupture event are detected, if no rupture events are fed into the force curves.

To determine the detection probability of a rupture event as a function of the external parameters, thousands of force curves were analysed as described above. This detection probability can be plotted versus the simulated rupture force for the rupture event and fitted by a sigmoidal function (Fig. 6). The graph is termed the cut-off function of a certain cantilever

$$\text{detection}_{\text{rate}} = \frac{1}{1+\exp\left(\frac{x_{\text{half}}-\text{force}}{\text{rate}}\right)} \tag{6}$$

x_{half} represents the value, where 50% of the rupture force events are detected. The slope is dependent on the polymer length, speed and the measured bandwidth. For the simulation in Fig. 6(a) a polymer length of 100 nm and a velocity of 200 nm/s was assumed.

Again, both polymer length and retract speed, but now in addition also the type of cantilever determine crucially the resolution limit of the whole system. The lower limit under optimum conditions was found to be 2.5 pN for the smallest Asylum Cantilever,[2] 3.7 pN for the Olympus Biolever B[3] and 8.1 pN for the standard C-Veeco[4] cantilever. Small cantilevers are obviously needed to catch unbinding events which are only

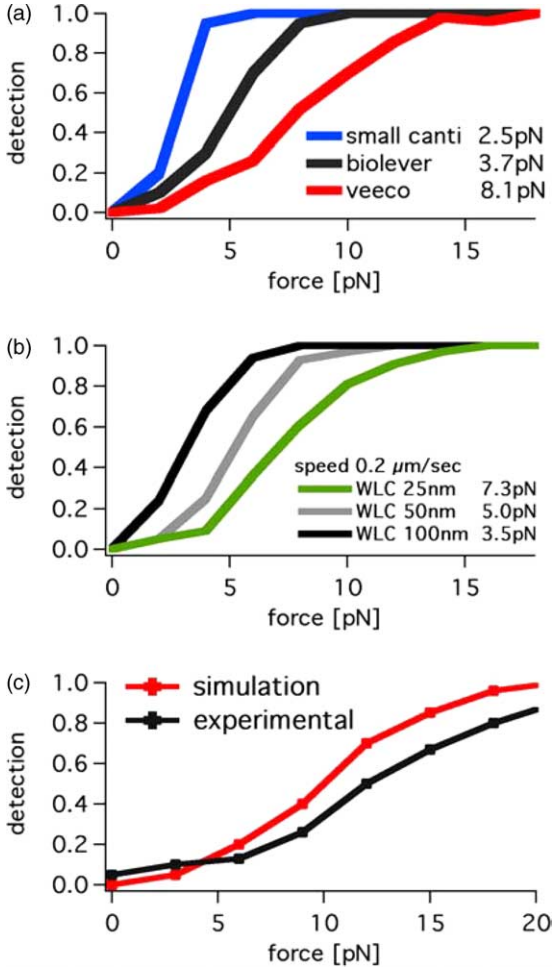

Fig. 6. (a) Cut off function for different cantilevers retracted at a speed of 200 nm/s and a 100 nm long polymer spacer. The red curve reflects the statistical resolution limit for a Veeco C cantilever, with a spring constant of 10 pN/nm. Events with 8.1 pN can be detected with a 50% likelihood, with is called the x-half value. The black curve is for an Olympus Biolever with 6 pN/nm and a x_{half} value of 3.7 pN. The blue curve is the simulation for a new small prototype cantilever of Asylum research. The x_{half} value is 2.5 pN. (b) Cut off function for different polymer spacer lengths. Longer spacers have lower frequencies in the PSD. Therefore, thermal noise can be separated more efficiently. (c) Comparison between simulation and experiment. The experimental cut off function was measured for the dsDNA binding protein LeXa. Additional factors like drift and instrumental noise lower the measured detection probability below the values obtained in the simulation.

a few piconewton in amplitude (Fig. 6(a)) and the spacer should be shorter than 50 nm at a speed of 1 μm/s. At a constant piezo velocity, the longest spacer performed best (Fig. 6(b)). This can be rationalized as follows: the longer spacer can be filtered with a lower corner frequency (Fig. 4(b)) and as a result thermal noise is more efficiently suppressed. Additional a longer spacer has a history of sampled data points, which results in a more effective analysis.

6. Polymeric anchors in bond rupture experiments

Up to now only the detection was optimized and the role of fluctuations in the signal was investigated, not the mechanism of the bond rupture itself, where fluctuations, both thermal and

[2] Asylum Research, Santa Barbara, CA, USA. Prototype cantilever (dimensions, 5×40 μm×80 nm; spring constant, 6 pN/nm; resonant frequency$_{\text{water}}$=10 kHz).

[3] Olympus Biolevers, BL-RC150VB. (dimensions, 30×100 μm×300 nm; spring constant, 6 pN/nm; resonant frequency$_{\text{water}}$=2–3 kHz).

[4] Veeco Instruments GmbH, Mannheim, Germany, MLCT-AUHW. (dimensions, 320×320 μm×500 nm; spring constant, 10 pN/nm; resonant frequency$_{\text{water}}$=0.8 kHz).

mechanical play a crucial role. Since most biologically relevant interactions are comparable in strength to thermal energies, force-induced processes like the separation of receptor–ligand system or the unfolding of a single molecule are fluctuation-assisted processes. The external applied force reduces the energy barrier, which the ligand has to overcome for dissociation [22,23]. As rupture event the external applied force is detected, at which the thermal induced dissociations process above the reduced energy barrier takes place. Therefore, the measured dissociation force reflects a force distribution, which is reduced and broadened by thermal fluctuations. This force distribution is characteristic for the potential landscape of the examined receptor–ligand system. The loading rate has to be taken into account, with which the receptor–ligand system is loaded or applied with force. Low loading rates give the dissociation process more time to overcome the energy barrier and, therefore, leads to higher possibilities for small rupture events and results in a low-force distribution. So it is possible to shift a force distribution to lower values by lowering the applied loading rate on the receptor–ligand system. Eq. (7) shows the correlation between the maximum of the force distribution (F^*) and the loading rate ($\dot{F}$) [24]

$$F^*(\dot{F}) = \frac{k_B T}{\Delta x} \ln\left(\frac{\dot{F}}{k^*_{off}} \frac{\Delta x}{k_B T}\right) \tag{7}$$

where Δx is the potential width and k^*_{off} the dissociation rate at no force. The maximum of the force distribution is directly proportional to the natural logarithms of the loading rate. Eq. (8) enables to fit the higher force distribution with high-loading rates and obtain the intrinsic values of the receptor–ligand systems Δx and k^*_{off}:

$$p(F) = k^*_{off} e^{(F\Delta x)/(k_B T)} 1\dot{F} e^{-k^*_{off} \int_0^F e^{(F\Delta x)/(k_B T)}(1/\dot{f})df} \tag{8}$$

Applying the theoretical fit with the determent values to a force distribution with lower loading rates, results in a deviation in the lower force regime. Through this the resolution limit can be detected experimentally and the cut-off function can be evaluated.

These findings were compared with experimental results that were published in Kühner et al. [2], where we found that the unbinding force histograms for a dsDNA binding protein (LeXa) deviated significantly from the calculated distribution in the low force regime. This was attributed to the instrument cut-off caused by the crossover between unbinding and thermally driven cantilever fluctuation. Comparing the experimental and the theoretical cut-off functions (Fig. 6(c)), it is obvious that the theoretical function gives a lower limit. In the experiment instrumental noise, sampling rates and drift, changing from experiment to experiment, additionally lower the resolution limit.

For this reason a reconstruction of an experimental cut force distribution is not possible. However, it is possible to fit Eq. (8) to the higher force regime of the distribution and obtain Δx and k^*_{off}. Neglecting different noises at altered speeds, because of diverse adjusted low pass filters, (Fig. 4) the width of the force distribution, which correlates inverse to Δx, is the same for varied loading rates. For an additional barrier Δx_2 at higher loading rates [25,26] in the receptor–ligand system the width of the force distribution gets broadened.

7. Propagation of force fluctuations in polymers

An additional point to consider is the mechanical fluctuation (e.g. acoustically excited oscillations) of either the cantilever or the surface, which can couple into the molecular complex to be analyzed. The force fluctuations acting on the complex (Fig. 7) are alleviated by the elastic properties of the polymer spacer, which behaves non-linear (Fig. 3(a)). For higher forces and shorter polymers the elastic properties stiffen and so for the force fluctuation coupling into the sample increases. Force fluctuations can lead to a destabilization of the receptor–ligand system. The force distributions are broadened and shifted to lower values. Long molecular polymer spacers between the cantilever and the receptor–ligand system can absorb part of these force fluctuation.

Here we discuss the fluctuation propagation along the polymer in a phonon limited mechanism, with the rational behind, that in the higher force range [27], where molecular bonds are typically probed, the conformational freedom of the polymer is already largely restricted. We are aware of the fact that for lower forces a diffusion-mediated transport might be a more adequate description.

Such non-thermal force fluctuations are non-trivial disturbances, since they may be hidden by the low-pass filter properties of the cantilever. As we have learned in the first section, mechanical fluctuations at frequencies higher than the corner frequency of the cantilever are not detected in a normal experiment. However, resonances of the instrument may lead to pronounced oscillations in the tip-surface distance and as such result in a periodic modulation of the loading force of the molecular complex under investigation (Fig. 8). They may be traced (but not measured) by recording the deflection spectrum of the cantilever in contact with the sample surface. A non-ideal vibration isolation may easily lead to a pronounced

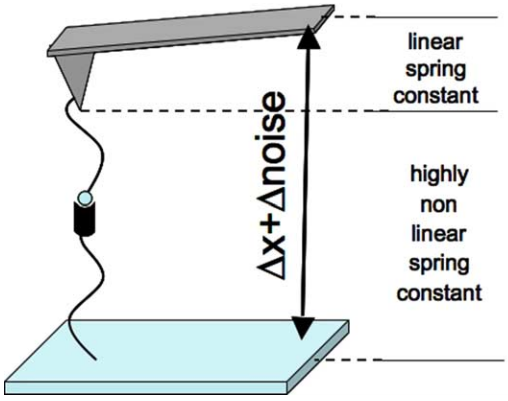

Fig. 7. Typical setup for force measurement of a receptor–ligand complex by AFM. Length fluctuation by mechanical noise cause force fluctuations acting via the polymeric spacers on the receptor–ligand system.

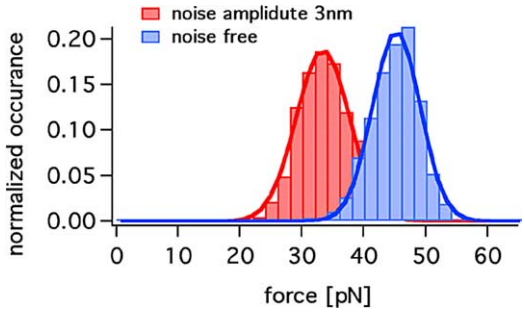

Fig. 8. Force distribution histograms of a 20 bpDNA in shear geometry derived in a Monte Carlo Simulation with a 20 nm polymer spacer. The red distribution depicts a simulation of the receptor–ligand system with 3 nm mechanical noise amplitude, the blue one with none.

excitation of vibrational modes of the instrument, which result in a modulation of the tip sample distance on the order of several nanometers. It is this kind of noise which is discussed in the following.

Forced unbinding events, like the ligand–receptor complexes ssDNA–ssDNA [14] or the unfolding of titin [28,29] domain, were simulated and histograms from thousands of events were collected as described above. The envelope of these histograms agreed well with the analytical expression derived by Evans et al. [24].

In a second set of simulations, a periodic modulation of the position of the sample surface, resulting in a modulation of the force acting on the complex was added. As was to be expected, the resulting histogram showed a pronounced shift towards lower forces (Fig. 8). The mechanical fluctuations supported the thermal fluctuations to dissociate the complex.

In Fig. 9, we analyzed the shift in the maximum of the histograms as a function of the noise amplitude for different

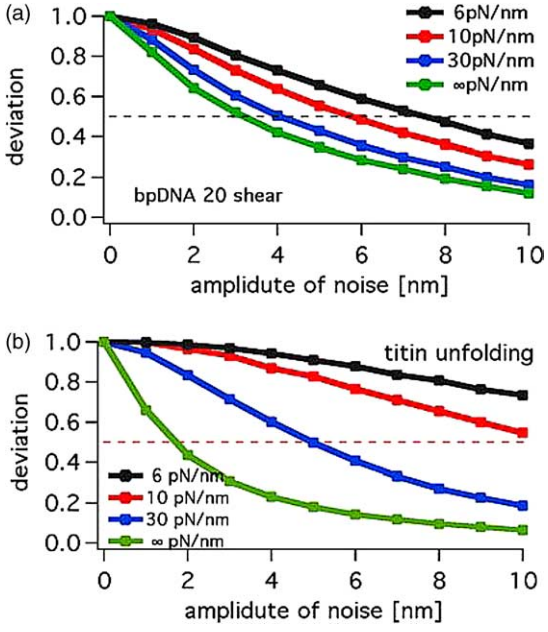

Fig. 9. Reduction of the maximum of the force distribution as a function of the added noise on the system for different cantilever stiffnesses. (a) For a 20 bpDNA in shear geometry. (b) For titin unfolding.

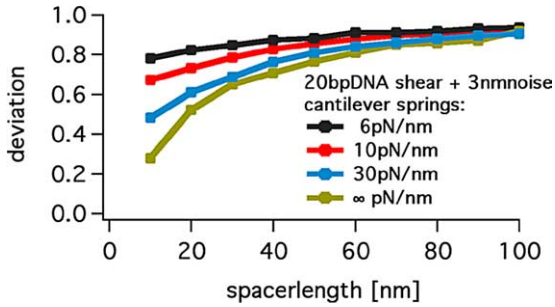

Fig. 10. Reduction of the maximum of the force distribution as a function of the polymer length for different cantilever stiffnesses at a noise amplitude of 3 nm. Long spacers soften the force fluctuations acting on the DNA complex.

cantilever stiffness. The result for a typical molecular system, DNA oligos is depicted in Fig. 9(a). The striking result is that already a noise amplitude of 4 nm reduces the apparent unbinding force by a factor of two, when a conventional cantilever with a stiffness of 30 pN/nm and a 20 nm length polymer are used

Titin—the other system under investigation (Fig. 9(b))—exhibited a much stronger stiffness dependence, because of its smaller potential width Δx

$$k_{\mathrm{off}}(F) = k_0^* \exp\left(-\frac{\Delta x F}{k_{\mathrm{B}} T}\right) \tag{9}$$

The dependence of this misreading of unbinding forces on the spacer length was analyzed in Fig. 10. As to be expected longer spacers and softer cantilevers weaken the effect of the length fluctuations. As a result, a 20 bpDNA oligo in shear geometry needs a 80 nm spacer and a soft cantilever to provide unbinding forces at an accuracy of $\pm 10\%$ if the noise floor is 3 nm.

In the well established force versus loading-rate plots (Fig. 11), which allow the direct extraction of potential width and off rate of the investigated complex, an increasing noise floor shows up in a reduction of the abscissa and as a result a pseudo-increased off rate! This finding is not counter-intuitive,

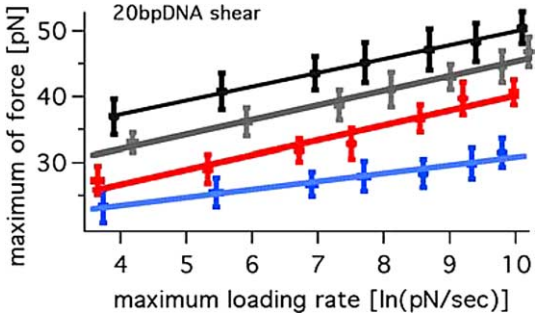

Fig. 11. Maximum of the force distribution as a function of the loading rate. The black curve is the noise free simulation for a molecular complex with a potential width and spontaneous off rate of $\Delta x = 2.0$ nm and $k_{\mathrm{off}}^* = 5 \times 10^{-7}\ \mathrm{s}^{-1}$. The spring constant was 30 pN/m. The grey and the blue curve were simulated with a 1 and 3 nm noise amplitude and resulted in apparent potential with and spontaneous off rates of $\Delta x = 1.9$ nm/$k_{\mathrm{off}}^* = 1.3 \times 10^{-5}\ \mathrm{s}^{-1}$ and $\Delta x = 3.4$ nm/$k_{\mathrm{off}}^* = 2 \times 10^{-7}\ \mathrm{s}^{-1}$, respectively. For the red curve a softer cantilever with 10 pN/nm spring constant was used and resulted in $\Delta x =$ 1.8 nm and a $k_{\mathrm{off}}^* = 1.7 \times 10^{-4}\ \mathrm{s}^{-1}$ at 3 nm noise amplitude.

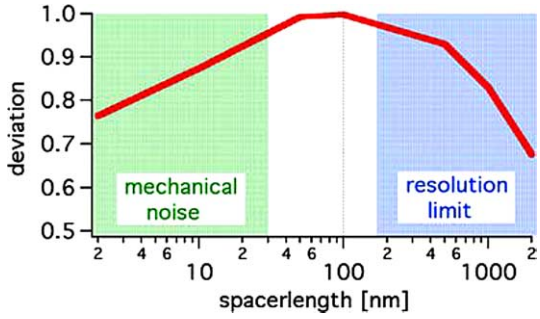

Fig. 12. Optimum spacer length for a receptor–ligand system with $\Delta x = 0.5$ nm and a $k^*_{off} = 0.1\ s^{-1}$ when a mechanical noise amplitude of 3 nm must be tolerated.

since the mechanical agitation of the complex enforces its dissociation.

These findings suggest that longer spacers are needed to reduce the influence of mechanical noise. On the other hand, Eq. (7) implies that the measured rupture force increases with higher loading rates at the molecular complex. At a given maximum retract speed, which is ultimately limited by the viscous drag on the cantilever, a maximum force rate, however, is limited by the spacer length. An optimum must, therefore, be found which compromises the above requirements. Fig. 12 shows the reduction of the measured force caused by mechanical noise and thermal fluctuation as a function of the spacer length. The simulation is performed with a pulling speed of 1 μm/s and is based on a receptor–ligand system with a Δx of 0.5 nm and a k^*_{off} of 0.1 s^{-1}. For such a system, the ideal spacer turns out to have a length between 50 and 100 nm.

Fig. 13 summarized the results and links them in a grossly oversimplified manner to other limitations of single molecule force spectroscopy. An ideal molecular complex with a single minimum in the energy landscape, whose dissociation is Markovian, gives rise to a straight line in the plot. The

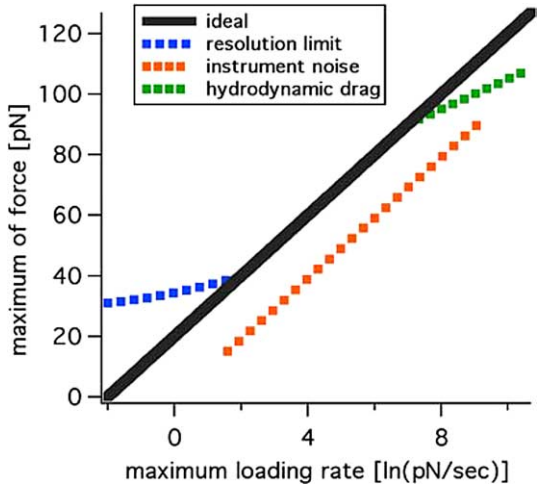

Fig. 13. Schematic representations of the different experimental limitations and the resulting deviations from the ideal situation.

hydrodynamic drag on the cantilever bends the curve at higher loading rates,[5] whereas drift and instrumentation noise lifts it at lower rates. A mechanical noise floor with increasing amplitude shifts it parallel to the force axis.

8. Concluding remarks

Small cantilevers have less damping and higher resonance frequencies. This obviously results in less noise in the desideratum bandwidth and, therefore, a better SNR. Mechanical fluctuations considerably reduce the measured rupture force of molecular complexes that are investigated by single molecule force spectroscopy. Polymeric anchors are, therefore, a necessity. Such polymer spacers reduce the force fluctuations of the cantilever but in turn reduce the force rate acting on the molecular complex and as a result again exceedingly reduce the measured rupture force. The optimum spacer length for typical ligand–receptor systems was found to be in the range of 50–100 nm.

Acknowledgements

This work was supported by the DFG. Helpful discussions with Thorsten Hugel, Matthias Erdmann, Richard Neher, Roger Proksch and Helmut Grubmüller are gratefully acknowledged.

References

[1] Rief M, Grubmuller H. Chemphyschem 2002;3:255–61.
[2] Kühner F, Costa LT, Bisch PM, Thalhammer S, Heckl WM, Gaub HE. Biophys J 2004;87:2683–90.
[3] Rief M, Gautel M, Gaub HE. Adv Exp Med Biol 2000;481:129–36 [discussion 137–41].
[4] Schwaiger I, Schleicher M, Noegel AA, Rief M. EMBO Rep 2005;6:46–51.
[5] Oesterhelt F, Oesterhelt D, Pfeiffer M, Engel A, Gaub HE, Muller DJ. Science 2000;288:143–6.
[6] Kessler M, Gaub HE. Structure (Camb); in press.
[7] Kessler M, Gottschalk KE, Janovjak H, Müller DJ, Gaub HE. J Mol Biol; in press.
[8] Kienberger F, Kada G, Mueller H, Hinterdorfer P. J Mol Biol 2005;347:597–606.
[9] Friedsam C, Wehle A, Kühner F, Gaub HE. J Phys: Condens Matter 2003;S1709–S23.
[10] Dammer U, Hegner M, Anselmetti D, Wagner P, Dreier M, Huber W, et al. Biophys J 1996;70:2437–41.
[11] Moy VT, Florin EL, Gaub HE. Science 1994;266:257–9.
[12] Zhang X, Chen A, De Leon D, Li H, Noiri E, Moy VT, et al. Am J Physiol: Heart Circ Physiol 2004;286:H359–H67.
[13] Clausen-Schaumann H, Rief M, Tolksdorf C, Gaub HE. Biophys J 2000;78:1997–2007.
[14] Strunz T, Oroszlan K, Schafer R, Guntherodt HJ. Proc Natl Acad Sci USA 1999;96:11277–82.
[15] Rief M, Oesterhelt F, Heymann B, Gaub HE. Science 1997;275:1295–7.
[16] Oesterhelt F, Rief M, Gaub HE. New J Phys 1999;6.
[17] Hugel T, Rief M, Seitz M, Gaub HE, Netz RR. Phys Rev Lett 2005;94:048301.

[5] Because of the non-linear velocity of the fast bended tip of the cantilever the hydrodynamic drag varies and result in a smaller detected force peak.

[18] Viani MB, Schaffer TE, Chand A, Rief M, Gaub HE, Hansma PK. J Appl Phys 1999;86:2258–62.
[19] Asylum research www.AsylumResearch.com.
[20] Putman CAJ, Grooth B-TGD, Hulst NFV, Greve J. J Appl Phys 1992;72:6–12.
[21] Lyons R. Understanding digital signal processing.: Prentice-Hall PTR; 1997.
[22] Evans E. Annu Rev Biophys Biomol Struct 2001;30:105–28.
[23] Evans E, Ritchie K. Biophys J 1999;76:2439–47.
[24] Evans E, Ritchie K. Biophys J 1997;72:1541–55.
[25] Merkel R, Nassoy P, Leung A, Ritchie K, Evans E. Nature 1999;397:50–3.
[26] Neuert G, Albrecht C, Pamir E, Gaub HE. FEBS Lett.; 2006; 580(2):505–9.
[27] Hallatschek O, Frey E, Kroy K. Phys Rev Lett 2005;94:077804.
[28] Oberhauser AF, Hansma PK, Carrion-Vazquez M, Fernandez JM. Proc Natl Acad Sci USA 2001;98:468–72.
[29] Rief M, Gautel M, Oesterhelt F, Fernandez JM, Gaub HE. Science 1997;276:1109–12.